DISCLAIMER

This report was prepared as an account of work sponsored by an agency of the United States Government. Neither the United States Government nor any agency thereof, nor any of their employees, makes any warranty, express or implied, or assumes any legal liability or responsibility for the accuracy, completeness, or usefulness of any information, apparatus, product, or process disclosed, or represents that its use would not infringe privately owned rights. Reference herein to any specific commercial product, process, or service by trade name, trademark, manufacturer, or otherwise does not necessarily constitute or imply its endorsement, recommendation, or favoring by the United States Government or any agency thereof. The views and opinions of authors expressed herein do not necessarily state or reflect those of the United States Government or any agency thereof. Reference herein to any social initiative (including but not limited to Diversity, Equity, and Inclusion (DEI); Community Benefits Plans (CBP); Justice 40; etc.) is made by the Author independent of any current requirement by the United States Government and does not constitute or imply endorsement, recommendation, or support by the United States Government or any agency thereof.

SANDIA REPORT
SAND20XX-XXXX
Printed Click to enter a date

Host Design for Carbon Capture and Regeneration in Porous Liquids

Jessica M. Rimsza, Brianna Addison, Nathan R. Bays, Colin McConnell, Sakun Duwal, Timothy Elmslie, Kimberly Haulenbeek, Matthew J. Hurlock, Sharlotte Kramer, Tina M. Nenoff, Harrison D. Root

Prepared by
Sandia National Laboratories
Albuquerque, New Mexico
87185 and Livermore,
California 94550

Issued by Sandia National Laboratories, operated for the United States Department of Energy by National Technology & Engineering Solutions of Sandia, LLC.

Available to DOE and DOE contractors from
U.S. Department of Energy
Office of Scientific and Technical Information
P.O. Box 62
Oak Ridge, TN 37831

Telephone: (865) 576-8401
Facsimile: (865) 576-5728
E-Mail: reports@osti.gov
Online ordering: http://www.osti.gov/scitech

Available to the public from
U.S. Department of Commerce
National Technical Information Service
5301 Shawnee Rd
Alexandria, VA 22312

Telephone: (800) 553-6847
Facsimile: (703) 605-6900
E-Mail: orders@ntis.gov
Online order: https://classic.ntis.gov/help/order-methods/

ABSTRACT

The demand for efficient gas capture technologies drives the exploration of porous liquids (PLs) as alternatives to traditional amine mixtures, which incur high operational costs due to energy-intensive regeneration processes. This research investigates the use of porous organic cages (POCs) within PLs to enhance gas capture and separation capabilities. We demonstrate that the flexibility of POCs under isostatic pressure facilitates the expulsion of captured gas molecules, enabling low-energy regeneration and the creation of an isostatic pressure testing capability for PLs. Additionally, a new CC3-OH POC derivative with scrambled hydroxides exhibits a twofold increase in CO_2 adsorption capacity, attributed to enhanced interactions between hydroxide linkers and CO_2. Furthermore, we explore the stability of azobenzene-containing organic cages formed via imine and amine bonds, revealing that the flexible amine bond allows for more efficient E-Z isomerization. Our findings highlight the transformative potential of PLs and azobenzene-derived systems in gas separation technologies, paving the way for innovative low-energy regeneration pathways.

ACKNOWLEDGEMENTS

This work was supported by the Sandia National Laboratories Laboratory Directed Research and Development program under project #230709. The authors thank Matthew S. Christian from Sandia National Laboratories for technical review of the report.

CONTENTS

LIST OF FIGURES

LIST OF TABLES

No table of figures entries found.

This page left blank

EXECUTIVE SUMMARY

The development of efficient gas capture and separation technologies is critical in addressing the growing demand for low-cost and energy-efficient solutions in industrial applications. Traditional methods, such as amine mixtures incur high operational costs due to energy-intensive regeneration processes. In contrast, porous liquids (PLs) have emerged as a promising alternative, offering permanent internal porosity and enhanced gas adsorption capacity. However, while the gas absorption properties of PLs have been evaluated, methods for their regeneration remain underexplored.

This research focuses on the innovative use of PLs, particularly those incorporating porous organic cages (POCs), to enhance gas capture capabilities. By employing computational material design alongside experimental synthesis, we have identified some of the key structural relationships that enable emergent properties in PLs. Our findings indicate that the flexibility of POCs under sufficiently high isostatic pressure can facilitate the expulsion of captured gas molecules, presenting a potential pathway for low-energy regeneration. Additionally, design and testing of a novel liquid pressure testing capability was completed, providing a path for a new liquid-phase testing capability at SNL.

Additionally, we have synthesized a new CC3-OH POC with scrambled linker hydroxides, resulting in a twofold increase in CO_2 adsorption capacity compared to traditional POCs. This emergent property is attributed to the free rotation of hydroxide linkers, which enhances interactions with CO_2 molecules. Furthermore, we explored the stability of azobenzene-containing organic cages formed via imine and amine bonds, revealing that the flexible amine bond allows for more efficient E-Z isomerization and greater stability in the Z configuration.

Overall, our research underscores the transformative potential of PLs and azobenzene-derived cage systems in gas separation technologies. By advancing our understanding of solvent interactions, mass transport properties, and binding site formation, we aim to develop innovative low-energy regeneration pathways that position PLs as a viable solution for environmental and industrial applications.

ACRONYMS AND TERMS

Acronym/Term	Definition
AML	Advanced Materials Laboratory
CC	Creative commons
DFT	Density functional theory
GPa	Gigapascal
LDRD	Laboratory Directed Research and Development
LVDT	Linear variable differential transformer
MEA	Monoethanolamine
MFC	Metal framework composite
MMEN	N,N’-dimethylenediamine
MOF	Metal-organic frameworks
PEA	Polyethyleneimine
PL	Porous liquid
PNNL	Pacific Northwest National Laboratory
POC	Porous organic cages
SNL	Sandia National Laboratories
TPB	1,3,5-triisopropylbenzene
ZIF	Zeolitic imidazolate framework

1. INTRODUCTION

Industrial separations and purifications account for 10-15% of the world's energy consumption, driving increased energy demand and cost[1]. Among purification processes, separation of contaminants from dilute gas streams, are particularly challenging and require highly selective and cost-efficient separation materials. Additionally, dilute separations often occur under different environmental conditions (temperature, pressure, relative humidity) compared to industrially produced gas streams (e.g., flue gases). Therefore, there is a need for materials for low cost, energy efficient separations from dilute gas streams.

PLs are comprised of discrete porous hosts that are suspended in a fluid whose molecules are sterically excluded from the internal pore space, forming stable and permanent porosity[2, 3]. PLs are classified into four types. Type I creates the internal porosity in the PL through engineering of solvent molecules so that they include an empty pore. One example is through surface modification of hollow silica nanospheres, that allow the resulting material to form as a liquid phase[4]. Type II PLs establish the porosity through solvation of a molecular cage structure, such as a porous-organic cage, into a solvent with sufficiently large molecular structures that is excluded from the interior porosity, typically through steric exclusion from traversing the pore window. An example composition is a CC13 POC suspended in 2-chlorophenol[5, 6]. Type III PLs are comprised of a nanoporous material particle, such as a MOF or a zeolite, that is suspended in a solvent which remains excluded from the pore of the solid. An example of a Type III PL is the ZIF-8 MOF with 2'-hydroxyacteophenone[7]. Finally, Type IV PLs are a traditionally nanoporous solid that can be engineered through incorporation of defects to exhibit a measurable viscosity, and therefore behaves as a liquid. A theoretical example is a highly defective ZIF MOF with partial coordination of the Zn-N bond[8]. Schematics of these PL types are included in Figure 1.

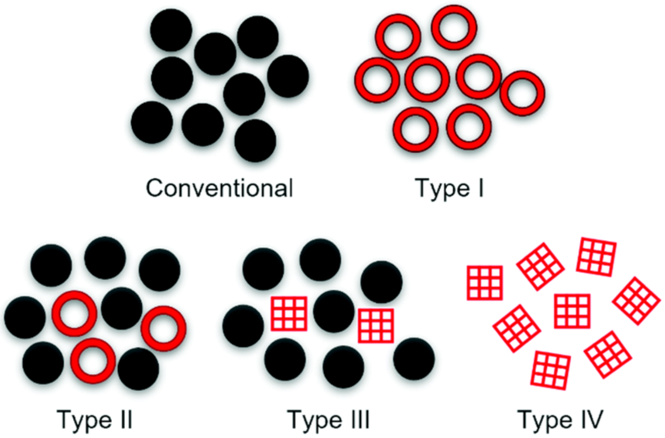

Figure 1: Schematic of PL types. Figure by Egleston et al. from Reference [9] licensed under CC BY 4.0

There are 500,000+ *potential* porous liquid combinations based on databases of candidate porous hosts and solvents, such as the coreMOF data base[10] and the PARIS III solvent database[11]. Therefore, traditional Edisonian approaches for creating new PL materials with targeted gas separation and adsorption properties is untenable to meet current technical demands. In this project, we applied computational material design with experimental synthesis and in-situ pressure experiments to accelerate the design of PLs as transformative, targeted materials for gas capture and separation. DFT molecular scale simulations were used to evaluate the structural flexibility and strength of CO_2 binding sites in POCs as model porous host structures. Changes in thermodynamic stability with isostatic compression will be calculated for POCs with the same morphology but different compositions to identify the source of POC compressibility. Candidate POCs were then synthesized, and in-situ micro-Raman spectroscopy and x-ray diffraction was used to confirm the structures. Adsorption isotherms and structural characterization were collected for the bulk POC and when it was formed into a PL through solvation in a stable silicone oil, Invoil704. Computational modeling of POC-gas binding was performed to identify how the difference in the structure of the POC altered CO_2 selectivity and adsorption capacity.

Currently, a critical roadblock in the use of liquid phase sorbent materials is the high regeneration cost[12]. This is driven by the formation of covalently bonded reaction products that need to be decomposed to allow for material regeneration. Previous work has suggested that it may be possible to regenerate PLs through the application of isostatic pressure, collapsing the pore structure and causing desorption of the gas molecules[13]. To date, the difficulties with placing the liquid-phase material under pressure has limited analysis. Therefore, we evaluated isostatic pressure regeneration mechanism using a custom-designed sample holder to carefully control pressure application and allow for quantification of the compressibility of PLs. The empty porosity of these systems provides a potential pathway for manipulating the properties of the material under pressure, a currently unknown feature of these novel materials.

2. ACCOMPLISHMENTS

2.1. Journal Articles

2.1.1. Published

Rimsza, J.M., S. Duwal, and H.D. Root. "Impact of vertex functionalization on flexibility of porous organic cages." *ACS Omega* (2024) 9, *24* 29025-29035 doi.org/10.1021/acsomega.4c04186 SAND2024-09481J

Root, H.D., Hurlock, M.J., Bays, N.R., Addison, B.M., and Rimsza, J.M. "Unlocking enhanced gas capture via core scrambling of porous-organic cages" *Journal of Molecular Liquids* (2025), 437, 128370 doi.org/10.1016/j.molliq.2025.128370

2.1.2. Submitted

Rimsza, J.M., Root, H.D., and Nenoff, T.M. "Untapped benefits of porous liquids for gas capture: low-energy regeneration" *Industrial & Engineering Chemical Research* (2025)

2.1.3. In-Preparation

Root, H.D., Goodman-Miller, S.A., Addison, B.M., Rimsza, J.M. "E-Z isomerization efficiency and stability changes through imine bond reduction in organic cages."

2.2. Post-Docs and Students

2.2.1. Post-Docs

Matthew J. Hurlock: Dr. Hurlock received his PhD in Chemistry from Washington State University and joined SNL in 2022. He supported this LDRD through formation and testing of the structure and properties of POC-based PLs. He is current a staff member at PNNL.

Timothy Elmslie: Dr. Elmslie received his PhD in Physics from the University of Florida and joined SNL in 2022. He supported this LDRD through pressure testing of synthesized POCs.

Nathan Bays: Dr. Bays received his PhD from the University of Missouri – Columbia in 2021 and joined SNL in 2023. He supported this LDRD through Matrix-Assisted Laser Desorption/Ionization Mass Spectrometry of the newly synthesized porous organic cage structures.

2.2.2. Student Interns

Brianna Addison (University of New Mexico): Brianna is an undergraduate intern in the AML at SNL and is working towards a Bachelor of Science in Chemistry at the University of New Mexico. She supported this LDRD through inorganic synthesis of porous organic cages.

Sydney Goodman-Miller (University of Nebraska Lincoln): Sydney was an undergraduate intern in the AML at SNL. She supported this LDRD through inorganic synthesis of porous organic cages and is currently pursuing a PhD in Chemistry from the University of Maryland.

2.3. Conference Presentations

Rimsza J.M., Duwal, S. and Root H.D., "Compression of Porous Organic Cages for Gas Capture", Fall 2023 ACS Meeting, San Francisco, CA

Root, H.D., Hurlock, M.J., Duwal, S., Elmslie, T., and Rimsza, J.M. “CC3 Porous Organic Cage Derivatives for Tailoring Properties of Porous Liquids” Fall 2024 ACS Meeting, Denver, CO

Rimsza, J.M., Hurlock, M.J., Bays, N., Addison, B., and Root, H.D. “Enhanced Gas Uptake in Porous Liquids Through Hydroxide Core Scrambling” Fall 2025 ACS Meeting, Washington DC

2.4. Awards and Intellectual Property

The porous liquid compositions and regeneration pathways developed through this project is protected under a patent application titled “Gaseous Absorption Compositions and Methods” under disclosure record number 16680.

Additionally, the impact of the porous liquid technology was recognized as a R&D 100 Award finalist for the technology titled “LEAP-L: Low-cost, low-Energy Absorption with Porous Liquids”. The graphical abstract of the R&D 100 Award application is included below as Figure 2.

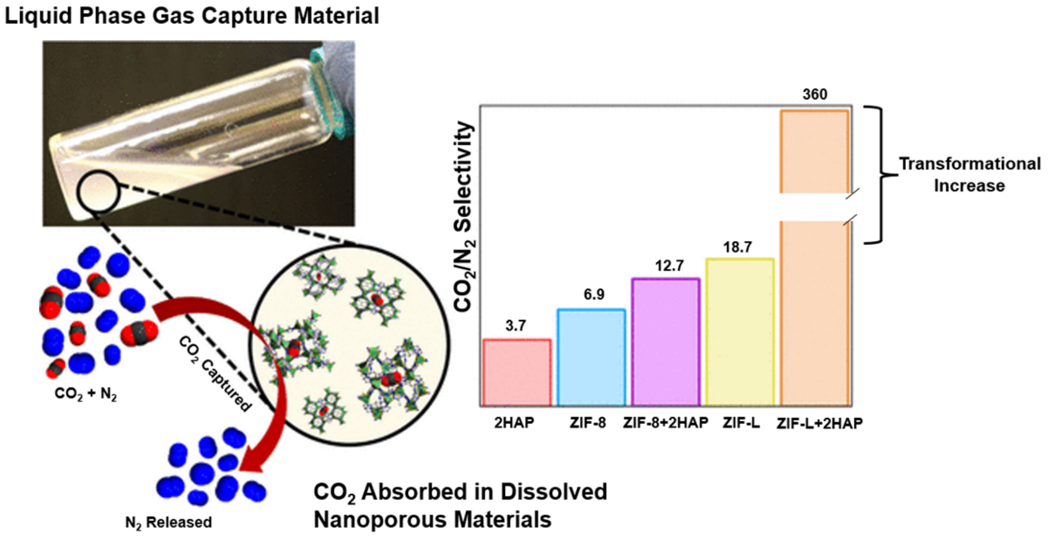

Figure 2: Graphical abstract of R&D 100 Award application demonstrating the transformational gas capture material ‘porous liquids’ composed of dissolved nanoporous host materials with permanent porosity that result in high absorption capacity and CO_2/N_2 selectivity and low-energy regeneration methods suitable for drop-in replacement for current liquid phase gas capture and separation infrastructure.

3. IMPACT OF VERTEX FUNCTIONALIZATION ON FLEXIBILITY OF POROUS ORGANIC CAGES

Full Reference[13]**:** Rimsza, Jessica M., Sakun Duwal, and Harrison D. Root. "Impact of Vertex Functionalization on Flexibility of Porous Organic Cages." *ACS Omega* 9, no. 26 (2024): 29025-29034. doi/10.1021/acsomega.4c04186. SAND2024-09481J

Full Abstract: Efficient carbon capture requires engineered porous systems that selectively capture CO_2 and have low energy regeneration pathways. PLs, solvent-based systems containing permanent porosity through the incorporation of a porous host, increase the CO_2 adsorption capacity. A proposed mechanism of PL regeneration is the application of isostatic pressure in which the dissolved nanoporous host is compressed to alter the stability of gases in the internal pore. This regeneration mechanism relies on the flexibility of the porous host, which can be evaluated through molecular simulations. Here, the flexibility of POCs as representative porous hosts was evaluated, during which pore windows decreased by 10–40% at 6 GPa. POCs with sterically smaller functional groups, such as the 1,2-ethane in the CC1 POC resulted in greater imine cage flexibility relative to those with sterically larger functional groups, such as the cyclohexane in the CC3 POC that protected the imine cage from the application of pressure. Structural changes in the POC also caused CO_2 adsorption to be thermodynamically unfavorable beginning at ∼2.2 GPa in the CC1 POC, ∼1.1 GPa in the CC3 POC, and ∼1.0 GPa in the CC13 POC as seen in Figure 3, indicating that the CO_2 would be expelled from the POC at or above these pressures. Energy barriers for CO_2 desorption from inside the POC varied based on the geometry of the pore window and all the POCs had at least one pore window with a sufficiently low energy barrier to allow for CO_2 desorption under ambient temperatures. The results identified that flexibility of the CC1, CC3, or CC13 POCs under compression can result in the expulsion of captured gas molecules.

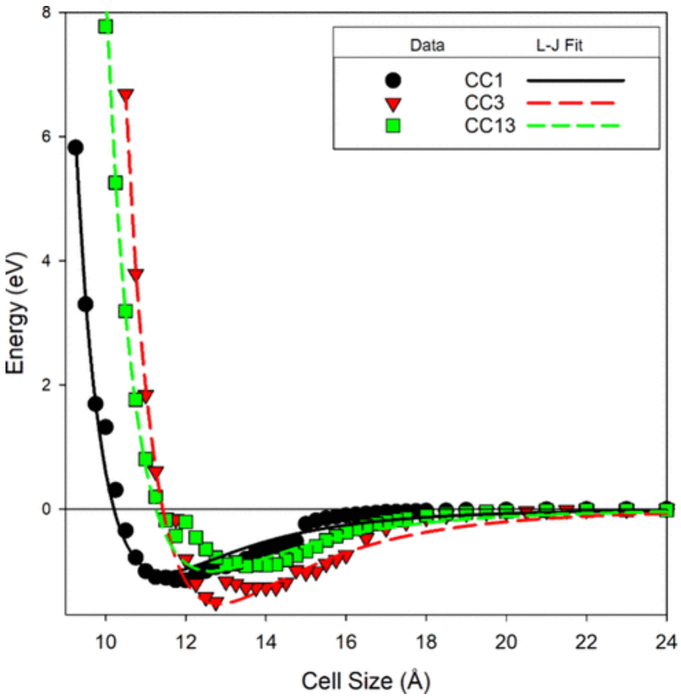

Figure 3: Change in energy (eV) will affect cell size (Å) for the three different POCs (CC1, CC3, and CC13) studied. Data are fit with a Lennard–Jones potential.

4. UNLOCKING ENHANCED GAS CAPTURE VIA CORE SCRAMBLING OF POCS

Full Reference: Root, Harrison D., Matthew J. Hurlock, Nathan R. Bays, Brianna M. Addison, and Jessica M. Rimsza. "Unlocking enhanced gas capture via core scrambling of porous-organic cages." *Journal of Molecular Liquids* 437 (2025): 128370. doi.org/10.1016/j.molliq.2025.128370

Full Abstract: The demand for low-cost, low-energy, and highly selective gas capture and separations is an ongoing driver of porous material development. PLs have been identified as a promising gas separation material by creating permanent porosity in inorganic solvents through inclusion of nanoporous materials that sterically exclude solvent from their internal porosity. Among the nanoporous materials that can be used to form porous liquids, POCs have been one of the most popular due to the inherent tunability of POCs. “Scrambled” POCs with varying functionalities on the POC vertices have been developed and incorporated into porous liquid compositions, increasing their gas adsorption capacity. An unexplored avenue to tailor the properties of porous liquids is through scrambling the functionality of the core of the POC. Therefore, we have synthesized a new POC, a CC3-OH derivative with scrambled hydroxides on the core and evaluated the impact on the CO_2 uptake capacity in silicon oil-based porous liquids. Core scrambling of the POC resulted in a twofold increase CO_2 adsorption capacity in the PL as seen in Figure 4, an emergent property that is a dramatic increase beyond a linear combination of the gas adsorption capacity of the neat solvent and the POC. DFT modeling of the CC3 POC and its hydroxide-based derivatives identified that free rotation of the linker hydroxide allowed for forced interaction between the CO_2 molecule and the hydroxide in the pore window. Solvation of the POC may release scrambled core hydroxides from intramolecular bonding with a neighboring imine, allowing for increased gas uptake in the porous liquid over the neat POC. These results identify a key structural relationship of POCs that enables emergent properties in porous liquids and can guide future development of liquid phase gas capture and separation materials for environmental and industrial applications.

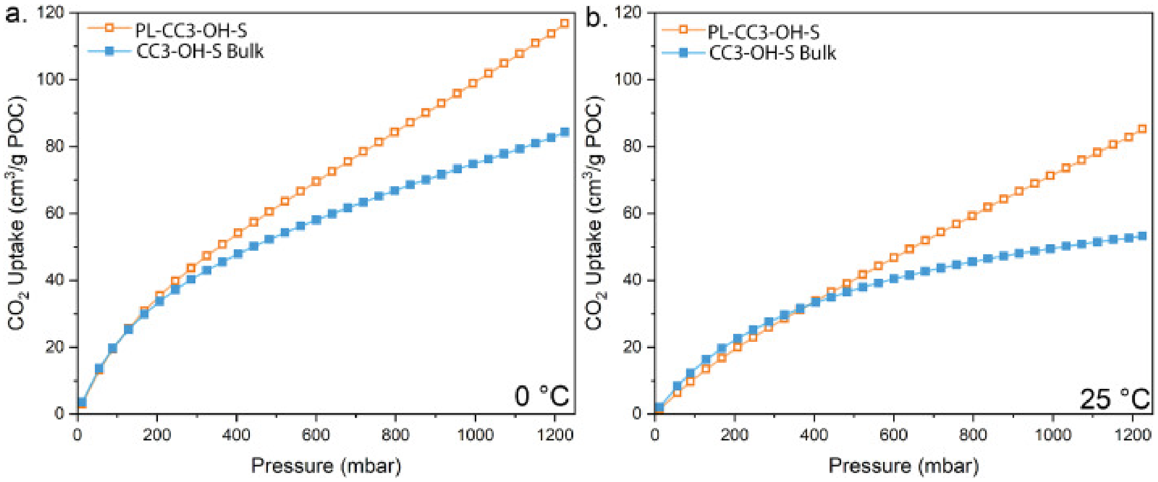

Figure 4: CO_2 uptake of bulk CC3-OH-S POC (solid blue squares) and in the 8.88 wt% CC3-OH-S + Invoil 704 PL (open orange squares) per-mass of the POC at (a) 0 °C and (b) 25 °C.

5. UNTAPPED BENEFITS OF PLS FOR GAS CAPTURE: LOW-ENERGY REGENERATION

Full Reference: Rimsza, Jessica M., Harrison D. Root, and Tina M. Nenoff "Untapped Benefits of Porous Liquids for Gas Capture: Low-Energy Regeneration" Industrial & Engineering Chemistry Research

Full Abstract: Current liquid-phase gas capture materials, such as amine mixtures, incur high operational costs due to the energy-intensive regeneration process creating a critical industrial need for alternative materials that retain the same engineering benefits while reducing energy requirements. Recently, porous liquids (PLs), liquid-phase materials with permanent internal porosity, have emerged as a promising replacement material with excellent gas absorption capacity and selectivity. Yet, despite evaluation of the gas absorption properties, potential methods for their regeneration, one of the critical potential benefits for their use over competing technologies, remains rare in literature. In this *Perspective*, we discuss not only the properties of PLs, but how further research is needed to understand solvent interactions, mass transport properties, and binding site formation that influences the ability of PLs to be regenerated. While conventional regeneration methods exist in PLs, and encouragingly take place at lower temperature than amine-based technologies as seen in Figure 5, the diverse compositions of PLs allow for the exploration of more efficient techniques and several approaches, including photosensitive azobenzene-based cage structures, isostatic compression, and sonication are discussed. Ultimately, the unique properties of PLs not only promise enhanced gas capture capabilities but also facilitate innovative low-energy regeneration pathways, positioning them as a transformative solution in gas separation technologies.

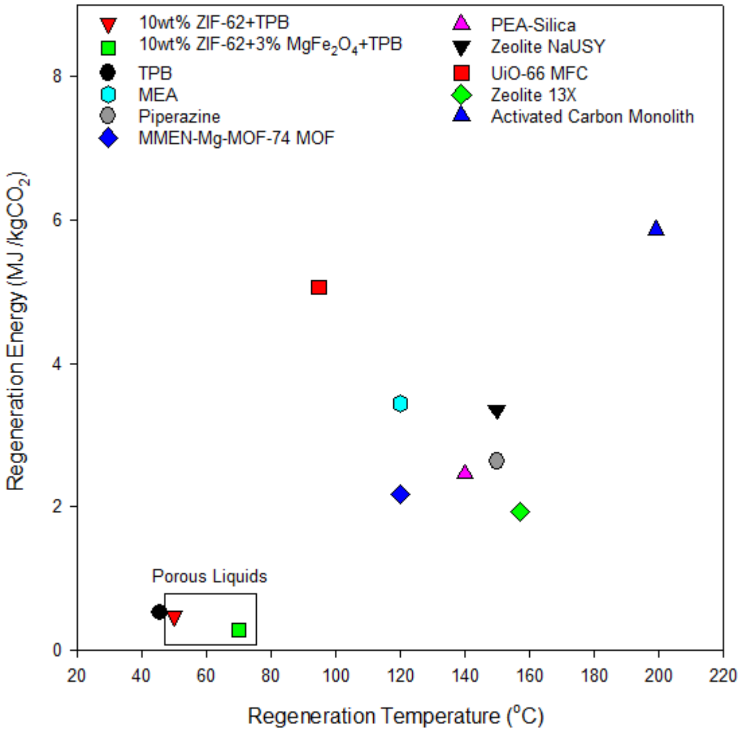

Figure 5: **Regeneration energy (MJ/kg CO_2) as a function of regeneration temperature for two ZIF-62 based Type III PLs (with and without magnetic nanoparticles), and comparison with literature values for solvents and solid sorbents. Data from Reference [14]**

6. E-Z ISOMERIZATION EFFICIENCY AND STABILITY CHANGES THROUGH IMINE BOND REDUCTION IN ORGANIC CAGES

Full Reference: Root, Harrison D., Sydney A. Goodman-Miller, Brianna M. Addison, Jessica M. Rimsza. "E-Z Isomerization Efficiency and Stability Changes Through Imine Bond Reduction in Organic Cages"

Full Abstract: Photoswitchable systems have found widespread utility in applications of chemical sensing, separations, and stimuli-responsive materials. Efficient use in these applications is predicated on low-energy and stable switching mechanisms that are robust and predictable. Azobenzene switching modalities have been explored in a variety of systems, including in organic cages. Organic cages with azobenzene components have been evaluated for the energetics of switching processes, but compositional impact on the resulting cage stability is underexplored. Herein, we report the differences in stability between azobenzene containing organic cages formed via either an imine or an amine bond. Not only does the flexible amine bond provide a more efficient E-Z isomerization as seen in Figure 6. Additionally, this provides stability to the Z configuration with no spontaneous Z-E isomerization, as is observed with imine-containing cages. DFT modeling on the Z and E isomers of the azobenzene cages identify energetics of transfer between the isomers, differences in the pore structure, and predicts the impact on their use in gas separations. The results demonstrate the tunability of azobenzene-derived cage systems as a pathway towards tunable organic molecules for gas separations.

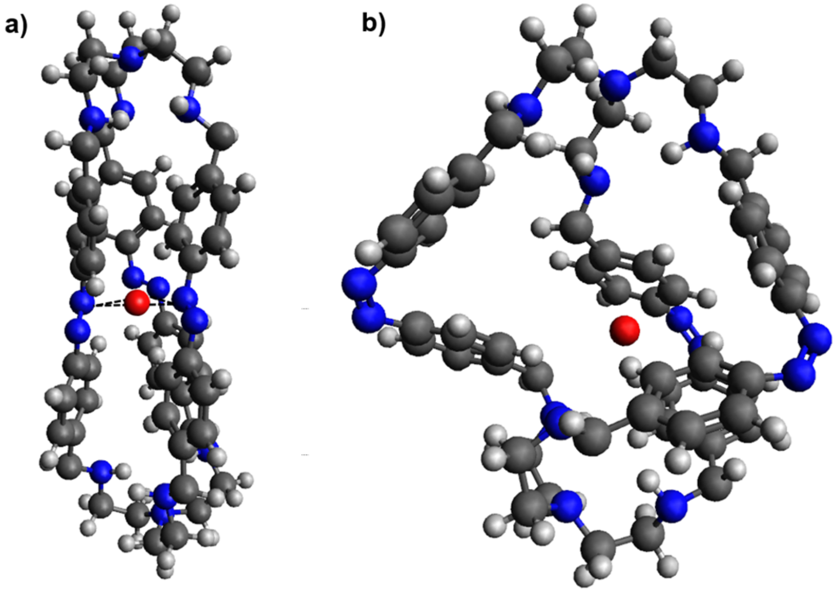

Figure 6: Snapshots of optimized azobenzene cage structure with amine linkages in the (a) EEE and (b) ZZZ isomers. Red ball identifies the center of mass of the molecule. Atom colors: carbon (grey), nitrogen (blue), and hydrogen (white)

7. POROUS LIQUID COMPRESSIBILITY TESTING

The Structural Mechanics Laboratory at SNL developed a method to measure the compressibility of a fluid-powder mixture as a function of pressure. The fluid-powder mixtures of interest were PLs where pores in the powder molecules could absorb the liquid at high pressure, thus changing its compressibility characteristics as the pressure and volume are varied. A design was developed in which the PL would be placed in a cylinder with a piston compressing the sample in the cylinder, as shown conceptually in Figure 7. By using a uniaxial hydraulic load frame to push the piston into the cylinder, the force and displacement could be measured. Since the dimensions of the cylinder and piston would be known, the displacement could be used to calculate the volume of the PL in the cylinder. Similarly, the pressure that the fluid would experience could be calculated using the force on the piston and the cross-sectional area of the piston. Measurement of these quantities enables the calculation of properties including compressibility, bulk modulus (the inverse of compressibility), and stored energy. This task complements similar work[15], but with the goal of attaining higher pressures (up to 10,000 psig as opposed to ~7,250 psig) and investigating different PL systems. Post-test analysis may be used to evaluate whether the change in the PL mixture was reversible or irreversible as well as providing insight into the chemistry that took place during testing. This section describes the development of the testing method and fixture, the initial testing that found that the first design was unable to maintain pressure due to leaking at the seal, efforts to evaluate potential changes to the seal design, and proposed future work.

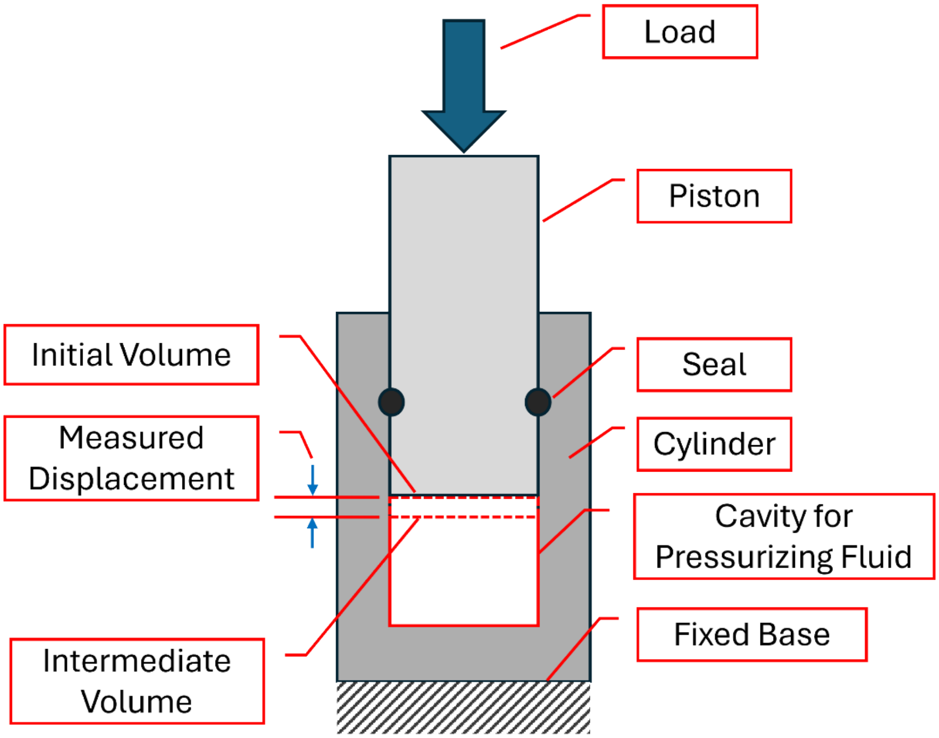

Figure 7: Schematic of Compressibility Tests

7.1. Fixture Design

A design was developed to conduct this testing, which is defined in drawing L02224 (please see Appendix A for drawings). Design goals included the ability to exceed the pressures attained in previous research, compatibility with an existing load frame that has a capacity of 22,500 lb-f, the ability to measure force (and thus pressure) throughout compression, the ability to accurately measure displacement (and thus volume), compatibility with a wide range of materials, the ability to minimize contamination of the sample with air, and a sample volume that is large enough to represent the bulk properties of the sample but small enough that it can be synthesized within a reasonable amount of time. A solid model of the compression fixture with a section view is shown Figure 8. A photo of the as-built fixture is shown in Figure 9. The fixture contains a cavity where the porous liquid sample may be compressed, and a high-pressure seal prevents leakage. The cavity has a nominal volume of 0.098 in^3 (~1.6 mL). The test fixture is designed to work at an operating pressure of 10,000 psi with a maximum allowable working pressure of 15,000 psi. The machined portions of the piston cylinder assembly that contact the sample are made of stainless steel 316 enabling maximum compatibility with different sample materials. A vent tube along the axis of the piston enables the removal of air bubbles from the sample while the stopper at the top of the tube will contain the pressure during testing. The desire to minimize the amount of air in the cavity led to the decision to eliminate items which could allow air bubbles to accumulate such as pressure sensors or pressure relief devices.

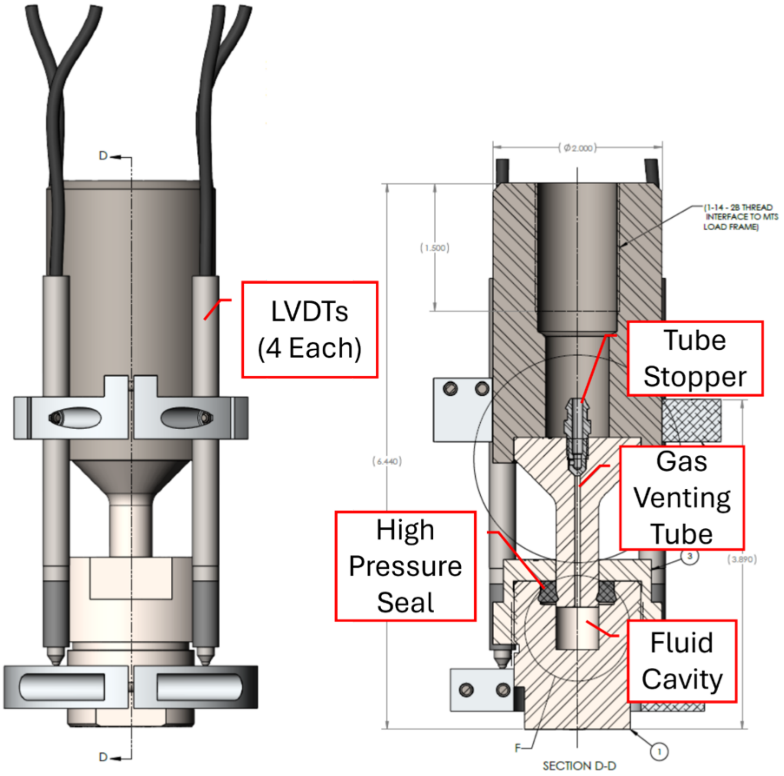

Figure 8: Solid Model of Porous Liquid Compression Fixture.

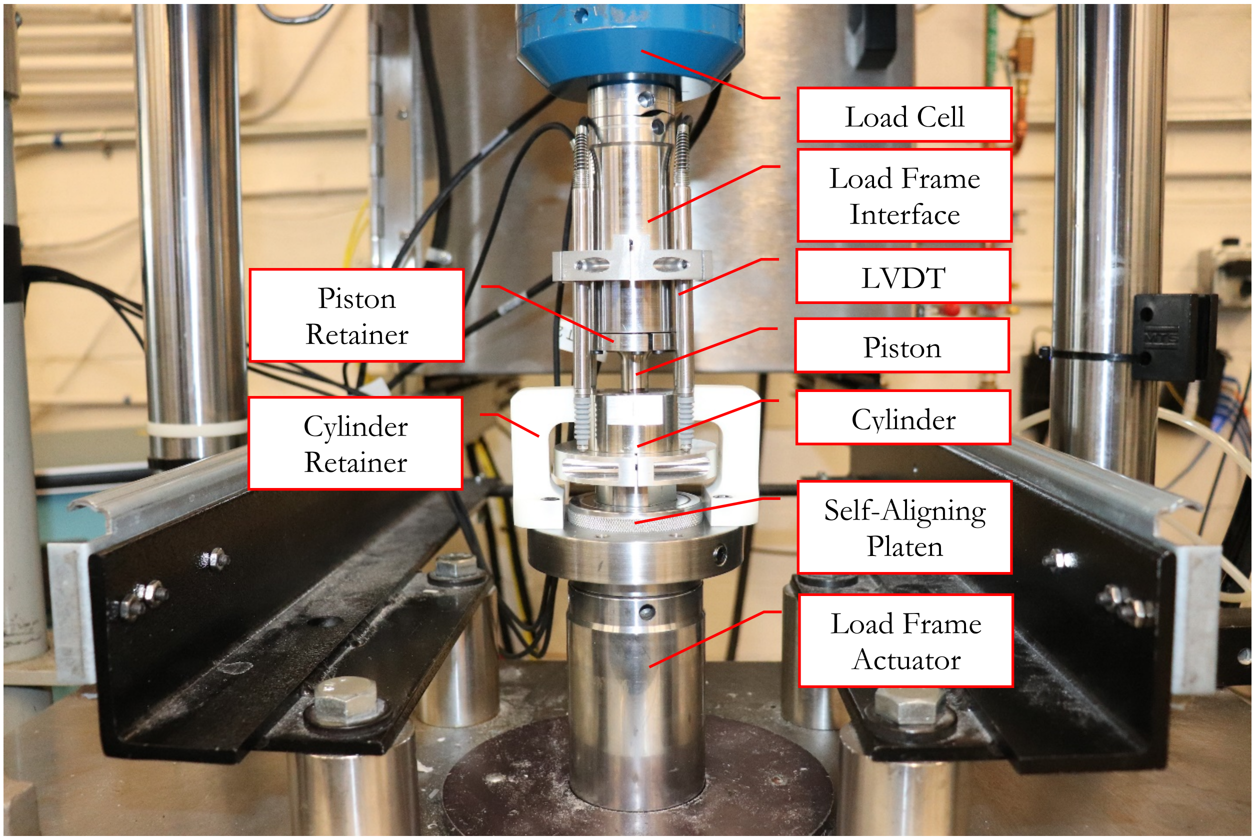

Figure 9. PL Compression Test Setup.

The compression fixture attaches to the load cell on the uniaxial load frame at the top with a threaded interface while the bottom is attached to compression platen which completes the load path on the load frame. Pressure is calculated by multiplying the force from the load cell by the cross-sectional area of the piston. The load corresponding to 10,000 psi is 1979.2 lb-f while the load corresponding to the maximum allowable working pressure of 15,000 psi is 2,943.8 lb-f, both well within the capacity of the load frame. Linear variable differential transformers (LVDTs) allow the precise measurement of the displacement of the piston, which ultimately enables the measurement of the sample volume. Four LVDTs are placed every 90 degrees about the axis of revolution of the fixture allowing measurement of any possible out-of-axis motion of the piston. The LVDTs are mounted to measure only the relative motion between the piston and cylinder, thus eliminating the possibility of including load frame compliance measurement in the volume calculation. The retainers for the piston and cylinder allow the piston to be withdrawn from the cylinder thus allowing the elimination of pressure stored within the cylinder.

7.2. Safety Considerations

There were numerous safety concerns that were addressed through design development and operational considerations. The main hazard that is introduced by this test method is pressure. The pressure hazard must be addressed during sample preparation, testing, and post-test sample handling.

After the sample is synthesized, it is placed in the sample cavity in the cylinder. The stopper is removed from the end of the vent tube in the piston, and the piston is inserted in the cylinder. Removing the stopper ensures that pressure cannot be generated in the sample. A press may be needed to facilitate initial insertion of the piston since the seal makes it resists the motion initially. As the piston is slowly inserted, air in the sample cavity and in the sample in the form of air bubbles are removed from the sample through the hole going through the axis of the piston. Once the air has been removed (as evidenced by liquid coming out through the hole in the piston), the stopper may be installed by screwing it into the top of the piston, and the sample is ready for testing.

During testing, the operator and any bystanders must be protected from the pressure hazard. To address safety concerns with pressurizing a liquid using a uniaxial hydraulic load frame, Pressure System Data Package PDP1520-SML-22 A 0 [2] was written and approved. The data package specifies 10,000 psig as the operating pressure with a maximum allowable working pressure of 15,000 psig. The system has a factor of safety of 1.8 at 10,000 psig and a factor of safety of 1.2 at 15,000 psig. A shielding system made of Unistrut and polycarbonate shielding was designed and built to protect the operator should rupture occur.

While testing on a uniaxial load frame, values such as pressure and stored energy were calculated. Limits on these values were included in the control software that would have caused the actuator to stop compressing the sample when safety limits were reached. For example, a pressure of 10,000 psig corresponds to a force of 1979.2 lb-f (found by multiplying 10,000 psi by the cross-sectional area of the piston). The program running the load frame was written to keep compressing the sample until a limit of 1950 lb-f at which point sample compression stops. The program was also written so that the actuator moves slowly, giving the operator more time to react should an undesirable condition occur while also allowing the sample to be compressed quasi-statically. The rate that was used was 0.0001 inch/second as opposed to 0.5 mm/minute which was used in[15] (which equates to 0.00033 inch/second).

Once the sample has been compressed to its final level, the actuator on the load frame slowly retracts the piston from the cylinder until the piston has returned to its original position. This removes stored pressure from the fixture thus making it safe for handling, enabling the sample to undergo post-test examination. The design was modified from the original drawings to include the ability to use the load frame to retract the cylinder from the piston, as seen in Figure 9, by adding the piston and cylinder retainers that allow the load frame to retract the piston from the cylinder.

7.3. Initial Testing

The test fixture underwent initial testing with water as a working fluid. The program worked well, and force increased to roughly 100 lb-f of compression (see Figure 10). Unfortunately, water was observed leaking past the seal, as shown in Figure 11. This likely accounts for the fact that the force oscillated and did not exceed roughly 100 lb-f. Because of the leakage, an investigation into how to effectively seal the enclosed volume was initiated.

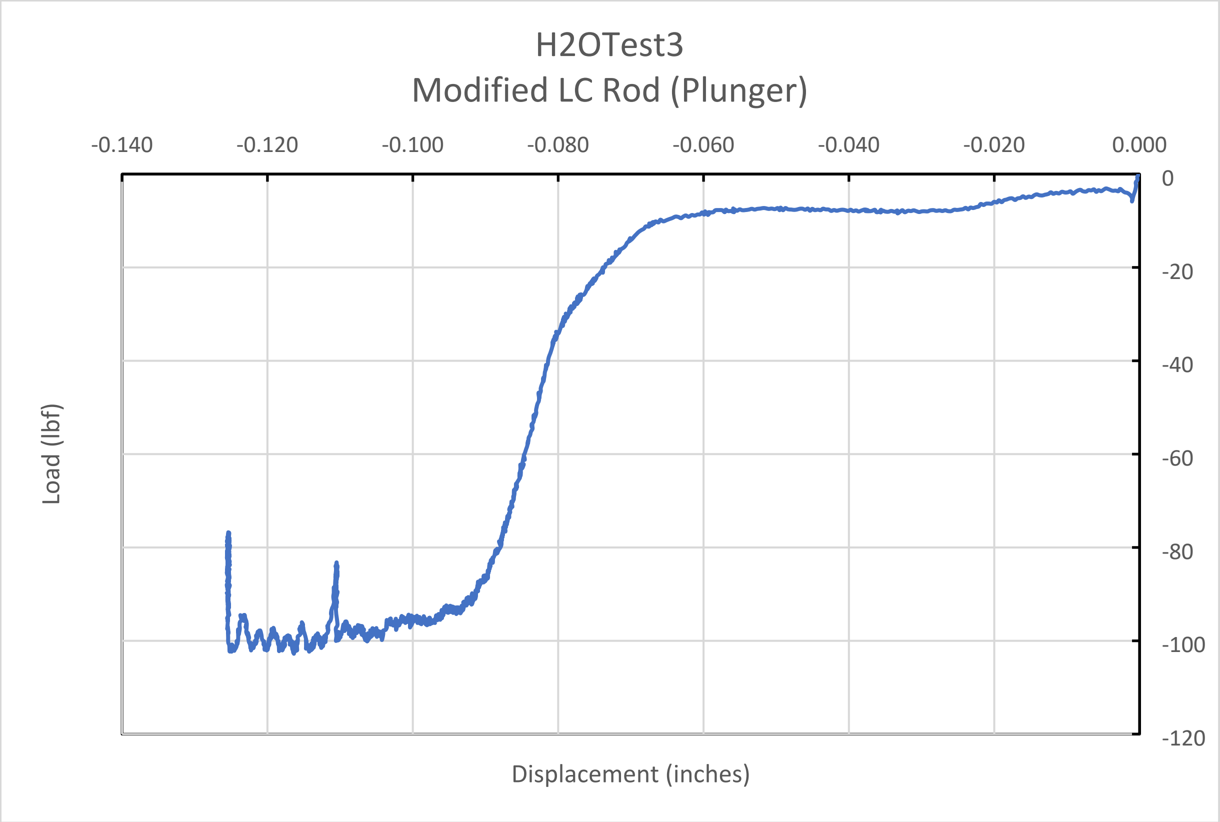

Figure 10. Force Versus Displacement for Water Testing Using Liquid Compressibility Fixture.

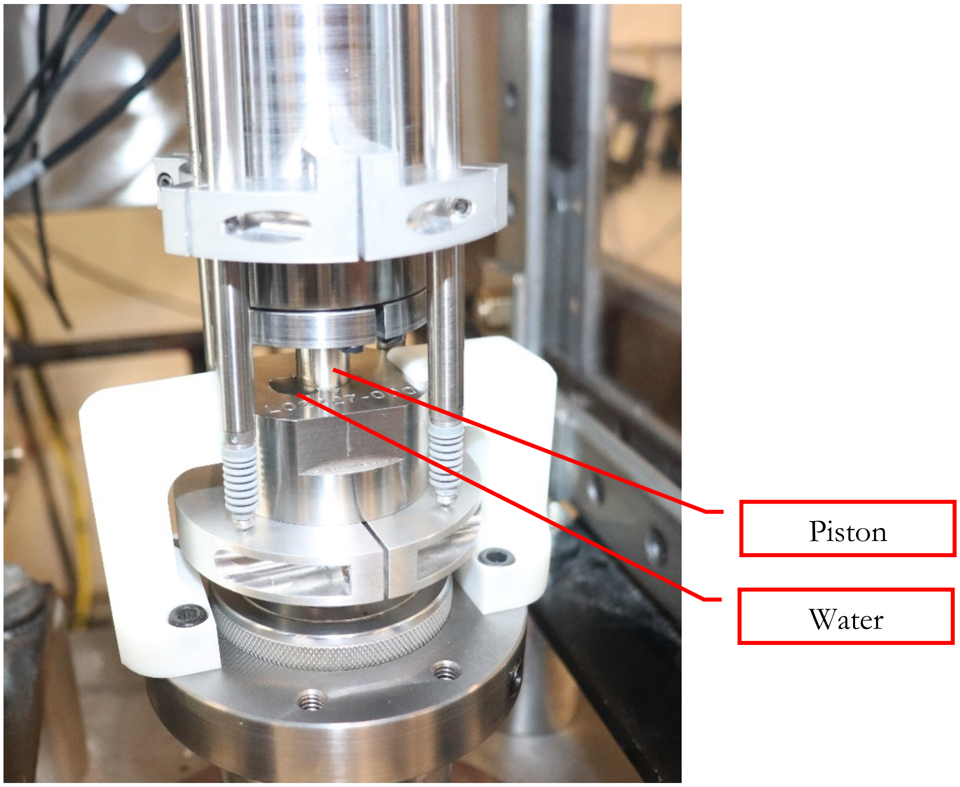

Figure 11. Water Leaking from Piston Seal During Initial Testing

7.4. Seal Details

The Sandia National Laboratories engineer who designed the fixture hardware also collaborated with engineers at American High Pressure Seals (AHPS), the vendor, to develop the high-pressure seal. Unfortunately, the Sandia engineer passed away at approximately the same time the fixture parts were being fabricated. With the engineer's passing, much of the details regarding the seal development was lost. The components from this design were fabricated and implemented for the initial testing. The initial check fit assembly of the fixture with the seal was performed by interpreting drawing number: 16675 (see Figure 12). This drawing was provided by the seal vendor, and was the only documentation found that appears to illustrate the seal assembly. Drawing interpretations used to for the initial assembly are displayed in Figure 12.

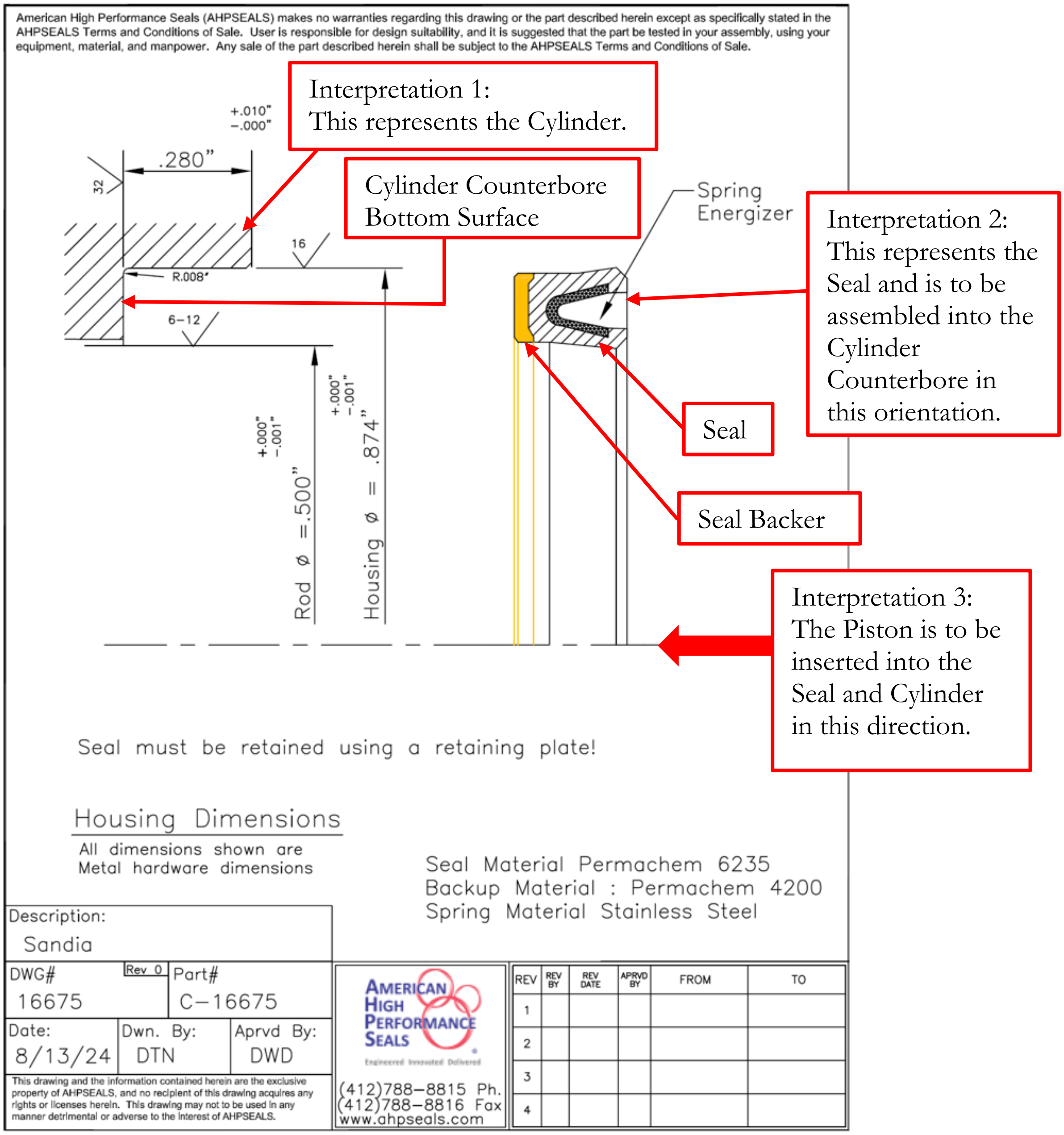

Figure 12. Drawing Number 16675 from Seal Vendor

During the initial assembly, it became apparent that the piston would not insert into the seal without damaging the seal. The seal engineer (Drew Nickelson) was contacted. The engineer advised to reverse the seal orientation so that the seal backer is not in contact with the bottom of the cylinder counterbore, and the piston is then inserted into the large side of the seal. It was also advised that a chamfer is required on the leading end of the Piston. A chamfer was subsequently added to the piston. The chamfer was not ideal, as the edges were sharp and unpolished (Figure 13e). The fixture was assembled according to the engineer's advice using a bench mount lever press to insert the piston. Water was added to the fluid cavity, and the test described in section "1.3 Initial Testing" was run. Fluid leaked from the fixture (Figure 11).

(a) Seal and Backer **(b) Seal Assembly** **(c) Initial Check Fit Assembly**

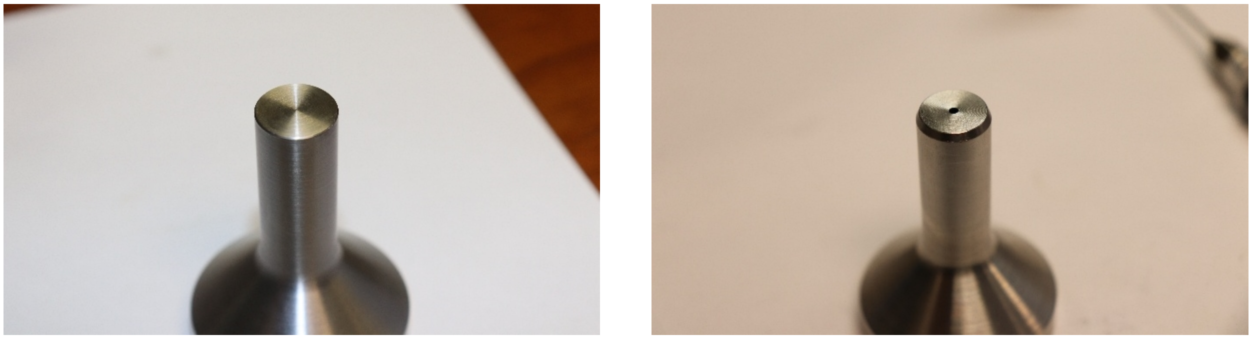

(d) Piston without Chamfer **(e) Piston with Chamfer**

Figure 13. Seal and Piston Components

A presentation to depict how the seals were being used in the test was prepared and sent to the seal vendor with the intention that the seals would be discussed to understand how to use them successfully. A new drawing (Figure 14 – Drawing Number: 16675INST) was received from Derek Duncan at AHPS. The drawing depicts specific features required for the seal to function successfully. Additionally, the vendor provided the following comments regarding how the seal functions:

- The open end containing the spring must face the pressure.
- The pressure must enter the spring groove of the seal to energize it.
- Ideally the piston should enter past the seal backer first.

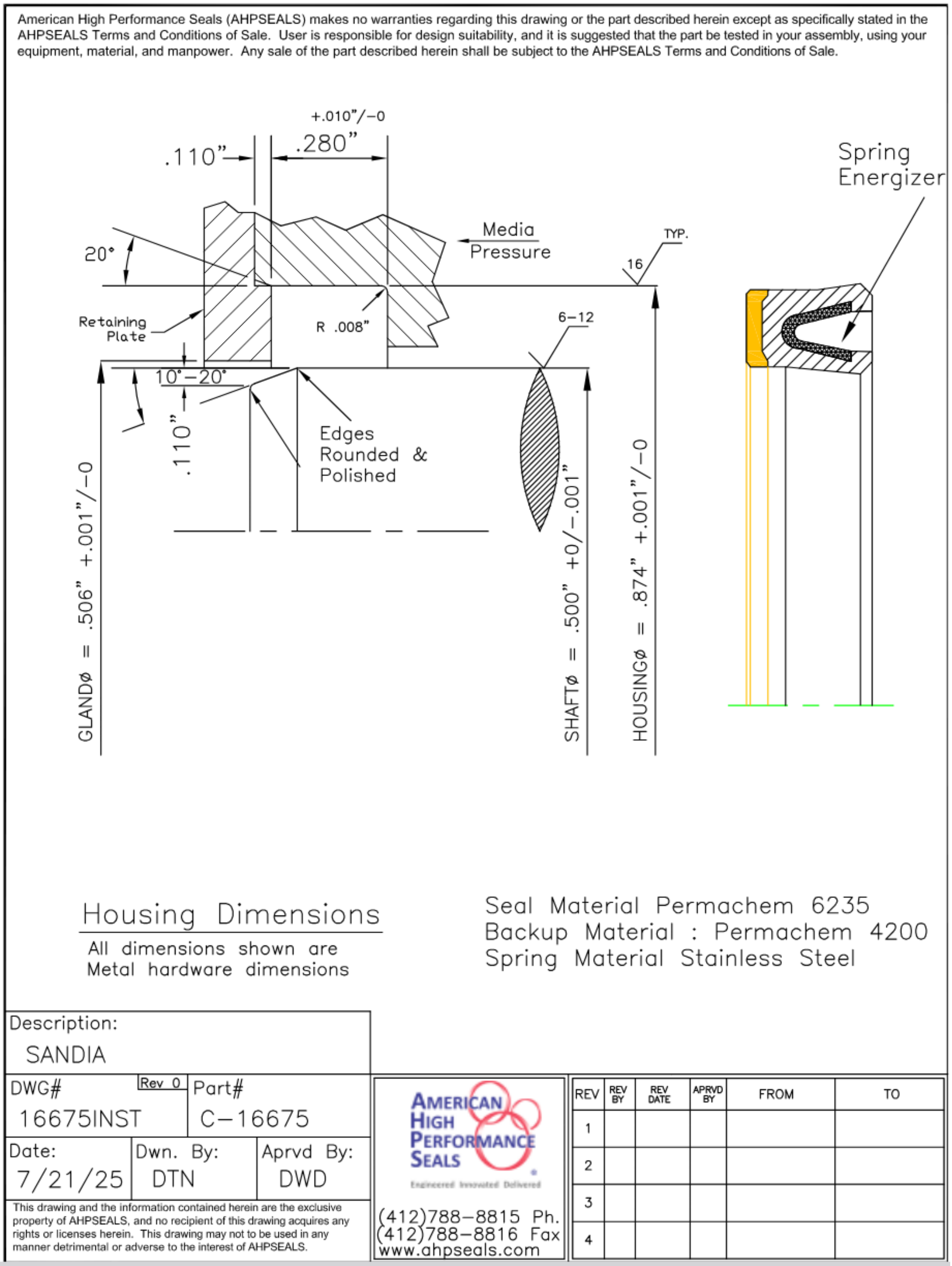

American High Performance Seals (AHPSEALS) makes no warranties regarding this drawing or the part described herein except as specifically stated in the AHPSEALS Terms and Conditions of Sale. User is responsible for design suitability, and it is suggested that the part be tested in your assembly, using your equipment, material, and manpower. Any sale of the part described herein shall be subject to the AHPSEALS Terms and Conditions of Sale.

Housing Dimensions

All dimensions shown are
Metal hardware dimensions

Seal Material Permachem 6235
Backup Material : Permachem 4200
Spring Material Stainless Steel

Description:
SANDIA

DWG# 16675INST
Rev 0
Part# C−16675
Date: 7/21/25
Dwn. By: DTN
Aprvd By: DWD

This drawing and the information contained herein are the exclusive property of AHPSEALS, and no recipient of this drawing acquires any rights or licenses herein. This drawing may not to be used in any manner detrimental or adverse to the interest of AHPSEALS.

(412)788−8815 Ph.
(412)788−8816 Fax
www.ahpseals.com

REV	REV BY	REV DATE	APRVD BY	FROM	TO
1					
2					
3					
4					

Figure 14. Drawing Number: 16675INST – Features Required for Seal to Function Correctly

7.5. Conclusions/Future Work/Lessons Learned

This design concept will enable measurement of fluid compressibility. This current design with the previously discussed modifications should work to ensure that pressure can be increased in the test cavity up to 10,000 psig.

There were several lessons-learned from this endeavor. First, one should not assume that a high-pressure seal will work as-is in this type of application, since this high-pressure system has many subtleties that are not present in typical sealing systems. Second, pressure safety design was extremely complex. The pressure safety package had to be extensive to cover all of the concerns. Third, potential hazards associated with the custom testing fixture presented themselves as the project went on. This included operational safety during sample preparation, test conduct, and removal of the sample from the test frame. Something that seems simple can actually be quite complex.

Here are recommendations for future work. First, modification or re-fabrication of all fixture hardware to the specifications prescribed in Drawing Number: 16675INST from American High-Performance Seals is needed to ensure that the design will allow the seal spring to be energized. Assembly of the fixture to specifications of Drawing 16675INST must be adhered to as to prevent damage to the seals and proper sealing, and the initial test with water is needed to assess seal performance. An investigation to learn if alternatives to this type of high-pressure seal exist may further improve the seal design. Once these actions are taken, this testing approach will be capability of testing up to the designed 10,000 psig.

REFERENCES

(1) Sholl, D. S.; Lively, R. P. Seven chemical separations to change the world. *Nature* **2016**, *532* (7600), 435-437.

(2) O'Reilly, N.; Giri, N.; James, S. L. Porous liquids. *Chemistry–A European Journal* **2007**, *13* (11), 3020-3025.

(3) Rimsza, J. M.; Nenoff, T. M. Porous liquids: computational design for targeted gas adsorption. *ACS Applied Materials & Interfaces* **2022**, *14* (16), 18005-18015.

(4) Shi, T.; Zheng, Y.; Wang, T.; Li, P.; Wang, Y.; Yao, D. Effect of pore size on the carbon dioxide adsorption behavior of porous liquids based on hollow silica. *ChemPhysChem* **2018**, *19* (1), 130-137.

(5) Rimsza, J.; Nenoff, T. M. Design of enhanced porous organic cage solubility in Type 2 porous liquids. *Journal of Molecular Liquids* **2023**, *377*, 121536.

(6) Chang, C.-W.; Borne, I.; Lawler, R. M.; Yu, Z.; Jang, S. S.; Lively, R. P.; Sholl, D. S. Accelerating solvent selection for type II porous liquids. *Journal of the American Chemical Society* **2022**, *144* (9), 4071-4079.

(7) Hurlock, M. J.; Lu, L.; Sarswat, A.; Chang, C.-W.; Rimsza, J. M.; Sholl, D. S.; Lively, R. P.; Nenoff, T. M. Exploitation of Pore Structure for Increased CO2 Selectivity in Type 3 Porous Liquids. *ACS Applied Materials & Interfaces* **2024**, *16* (38), 51639-51648.

(8) Bennett, T. D.; Coudert, F.-X.; James, S. L.; Cooper, A. I. The changing state of porous materials. *Nature Materials* **2021**, *20* (9), 1179-1187.

(9) Egleston, B. D.; Mroz, A.; Jelfs, K. E.; Greenaway, R. L. Porous liquids–the future is looking emptier. *Chemical science* **2022**, *13* (18), 5042-5054.

(10) Chung, Y. G.; Haldoupis, E.; Bucior, B. J.; Haranczyk, M.; Lee, S.; Zhang, H.; Vogiatzis, K. D.; Milisavljevic, M.; Ling, S.; Camp, J. S. Advances, updates, and analytics for the computation-ready, experimental metal–organic framework database: CoRE MOF 2019. *Journal of Chemical & Engineering Data* **2019**, *64* (12), 5985-5998.

(11) Harten, P.; Martin, T.; Gonzalez, M.; Young, D. The software tool to find greener solvent replacements, PARIS III. *Environmental progress & sustainable energy* **2020**, *39* (1), 13331.

(12) Nwaoha, C.; Beaulieu, M.; Tontiwachwuthikul, P.; Gibson, M. D. Techno-economic analysis of CO2 capture from a 1.2 million MTPA cement plant using AMP-PZ-MEA blend. *International Journal of Greenhouse Gas Control* **2018**, *78*, 400-412.

(13) Rimsza, J. M.; Duwal, S.; Root, H. D. Impact of Vertex Functionalization on Flexibility of Porous Organic Cages. *ACS Omega* **2024**.

(14) Ding, Y.; Zhao, X.; Qin, Y.; Zhu, X.; Cheng, M.; Wang, H.; Liao, Q. Desorption research and energy consumption assessment of a porous liquids impregnated by monoethanolamine (MEA). *Separation and Purification Technology* **2023**, *325*, 124626.

(15) Lai, B.; Liu, S.; Cahir, J.; Sun, Y.; Yin, H.; Youngs, T.; Tan, J. C.; Fonrouge, S. F.; Pópolo, M. G. D.; Borioni, J. L. Liquids with high compressibility. *Advanced Materials* **2023**, *35* (44), 2306521.

APPENDIX A. COMPRESSIBILITY TEST FIXTURE DRAWINGS

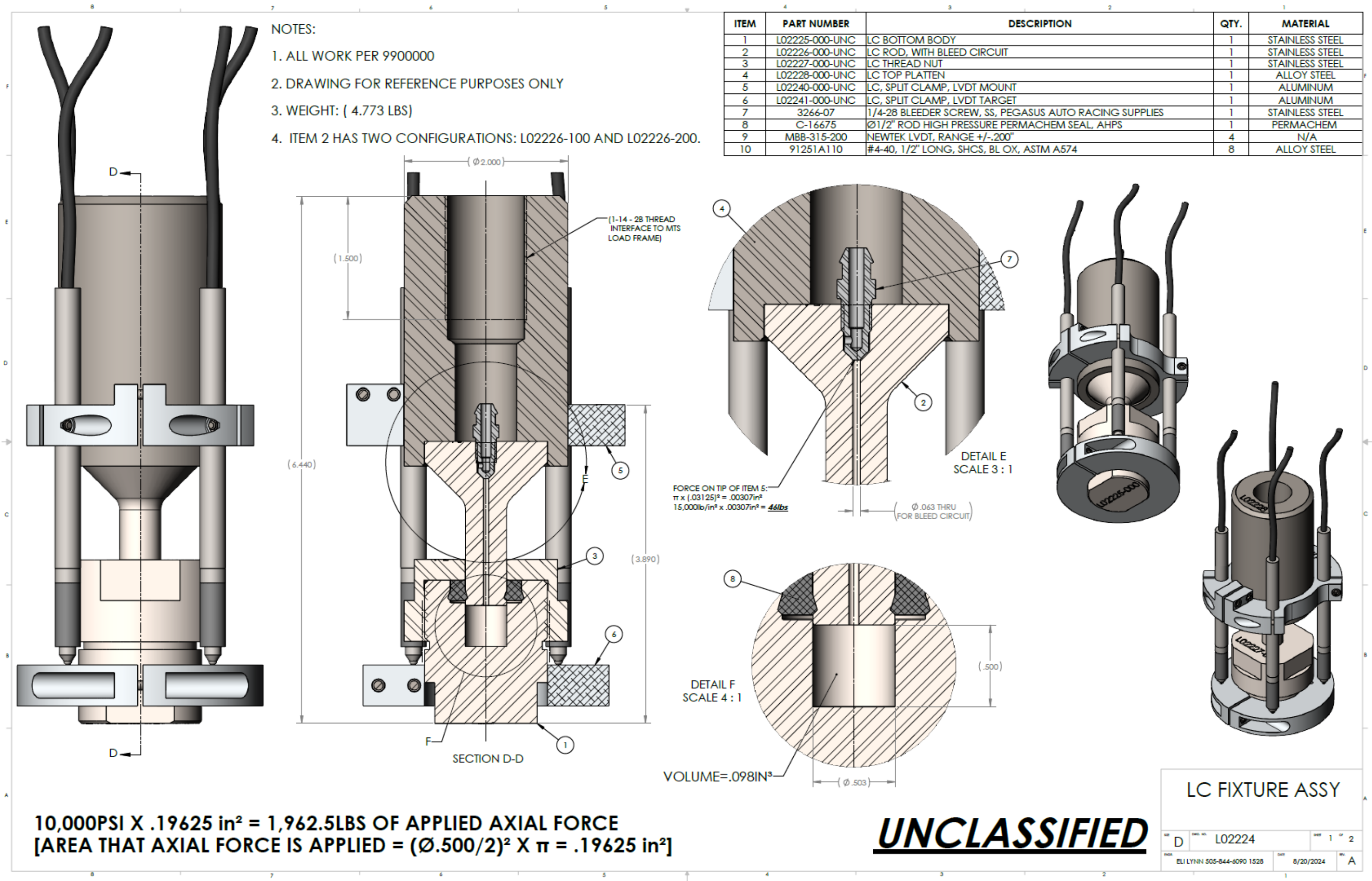

NOTES:

1. ALL WORK PER 9900000
2. DRAWING FOR REFERENCE PURPOSES ONLY
3. WEIGHT: (4.773 LBS)
4. ITEM 2 HAS TWO CONFIGURATIONS: L02226-100 AND L02226-200.

ITEM	PART NUMBER	DESCRIPTION	QTY.	MATERIAL
1	L02225-000-UNC	LC BOTTOM BODY	1	STAINLESS STEEL
2	L02226-000-UNC	LC ROD, WITH BLEED CIRCUIT	1	STAINLESS STEEL
3	L02227-000-UNC	LC THREAD NUT	1	STAINLESS STEEL
4	L02228-000-UNC	LC TOP PLATTEN	1	ALLOY STEEL
5	L02240-000-UNC	LC, SPLIT CLAMP, LVDT MOUNT	1	ALUMINUM
6	L02241-000-UNC	LC, SPLIT CLAMP, LVDT TARGET	1	ALUMINUM
7	3266-07	1/4-28 BLEEDER SCREW, SS, PEGASUS AUTO RACING SUPPLIES	1	STAINLESS STEEL
8	C-16675	Ø1/2" ROD HIGH PRESSURE PERMACHEM SEAL, AHPS	1	PERMACHEM
9	MBB-315-200	NEWTEK LVDT, RANGE +/-.200"	4	N/A
10	91251A110	#4-40, 1/2" LONG, SHCS, BL OX, ASTM A574	8	ALLOY STEEL

FORCE ON TIP OF ITEM 5:
$\pi \times (.03125)^2 = .00307\text{in}^2$
$15{,}000\text{lb/in}^2 \times .00307\text{in}^2 =$ ***46lbs***

10,000PSI X .19625 in² = 1,962.5LBS OF APPLIED AXIAL FORCE
[AREA THAT AXIAL FORCE IS APPLIED = (Ø.500/2)² X π = .19625 in²]

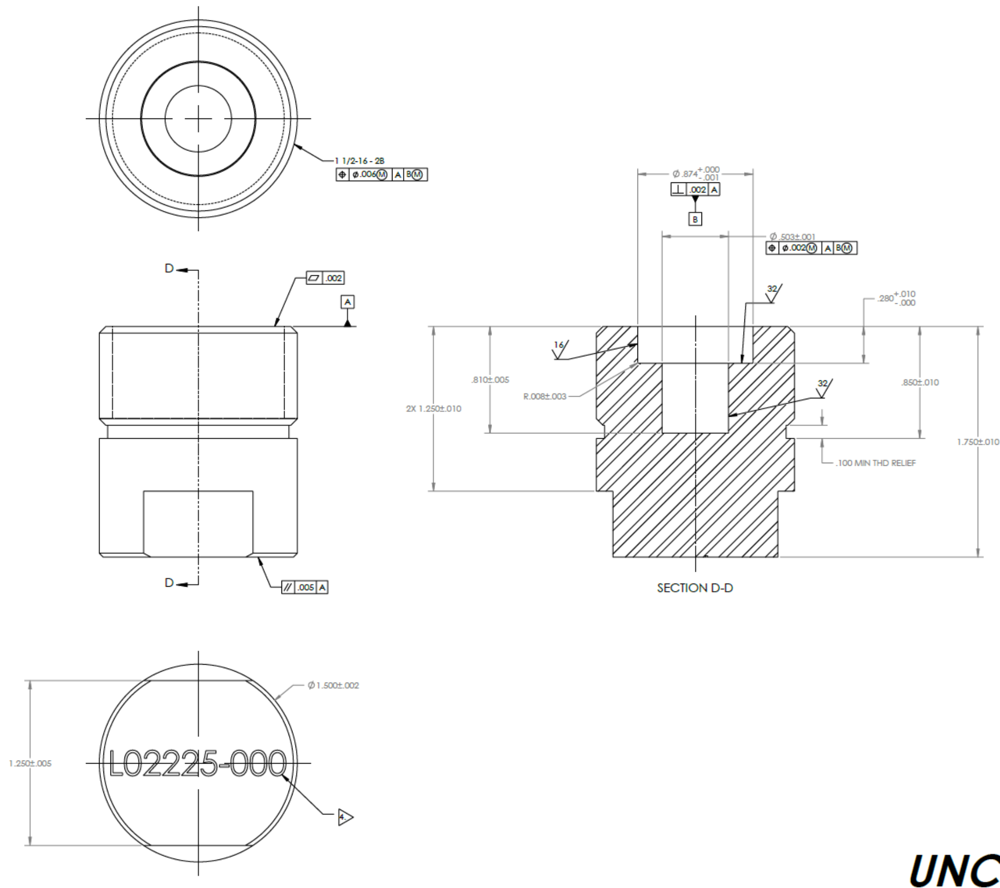

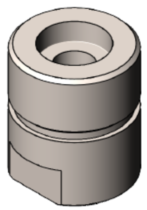

NOTES:

1. ALL WORK PER 9900000
2. MATERIAL: STAINLESS STEEL
   TYPE: 316
   HEAT TREAT: N/A
3. WEIGHT: (0.785 LBS)
4. MARK APPROX. AS SHOWN,
   APPROX. 3/16" FONT.
   LASER MARK OR ENGRAVE.

UNCLASSIFIED

LC BOTTOM BODY

SIZE D	DWG. NO. L02225	SHEET 1 OF 1
ENGR. ELI LYNN 505-844-6090 1528	DATE 8/19/2024	REV. A

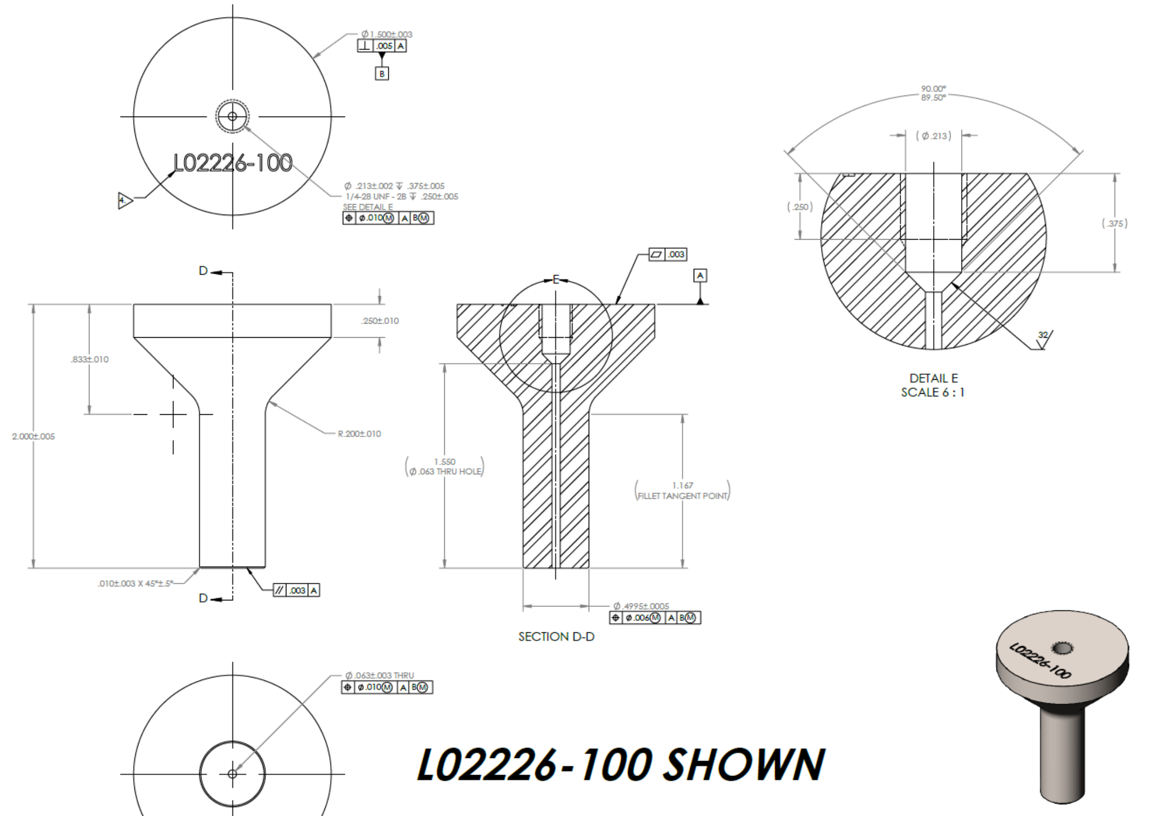

NOTES:

1. ALL WORK PER 9900000
2. MATERIAL: STAINLESS STEEL
   TYPE: 316
   HEAT TREAT: N/A
3. WEIGHT: (0.317 LBS)
4. MARK APPROX. AS SHOWN,
   APPROX. 1/8" FONT.
   LASER MARK OR ENGRAVE.

UNCLASSIFIED

LC ROD, WITH BLEED CIRCUIT			
SIZE D	DWG. NO. L02226	SHEET 1 OF 2	
ENGR. ELI LYNN 505-844-6090 1528	DATE 8/19/2024	REV. A	

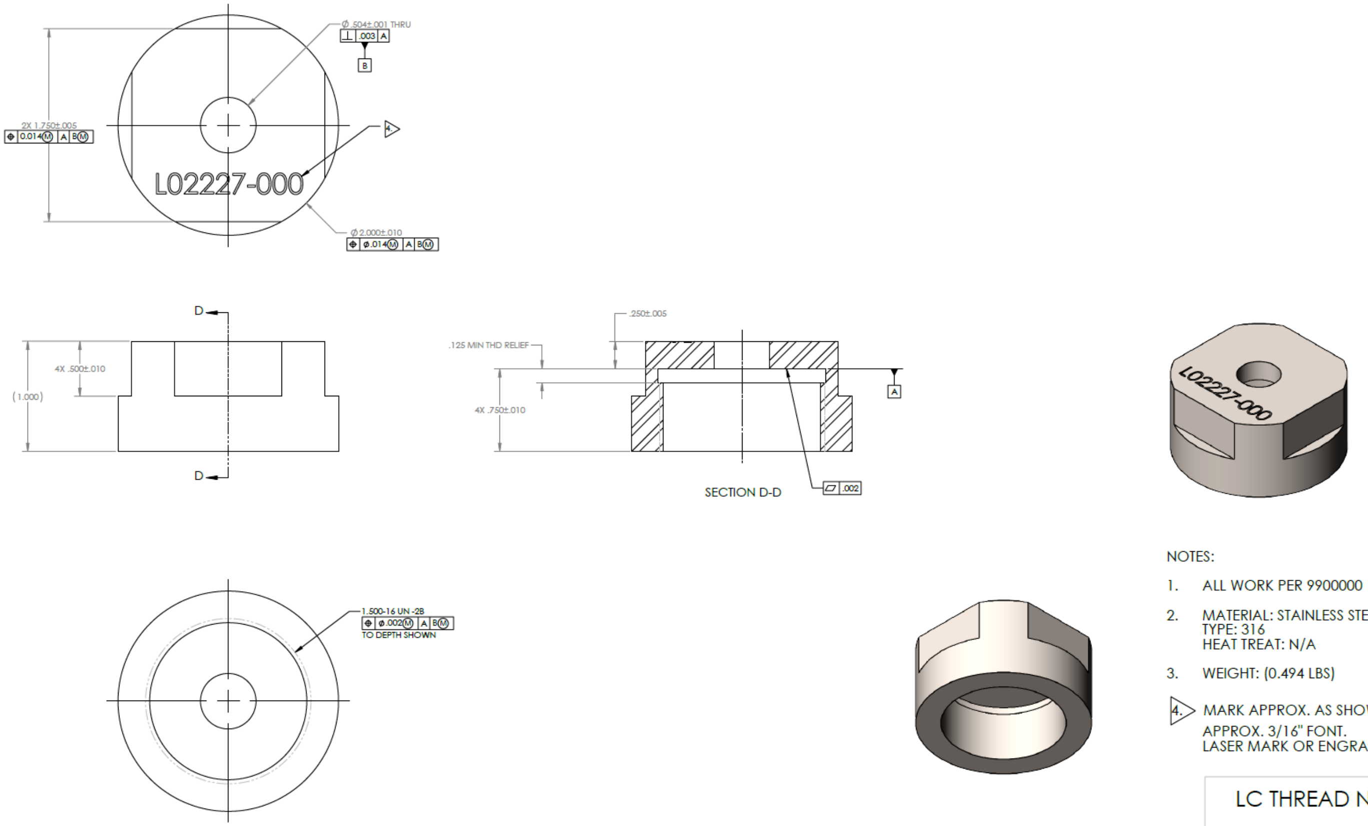

NOTES:

1. ALL WORK PER 9900000
2. MATERIAL: STAINLESS STEEL
   TYPE: 316
   HEAT TREAT: N/A
3. WEIGHT: (0.494 LBS)
4. MARK APPROX. AS SHOWN,
   APPROX. 3/16" FONT.
   LASER MARK OR ENGRAVE.

UNCLASSIFIED

LC THREAD NUT

SIZE D	DWG. NO. L02227	SHEET 1	OF 1
ENGR. ELI LYNN 505-844-6090 1528	DATE 8/19/2024	REV. A	

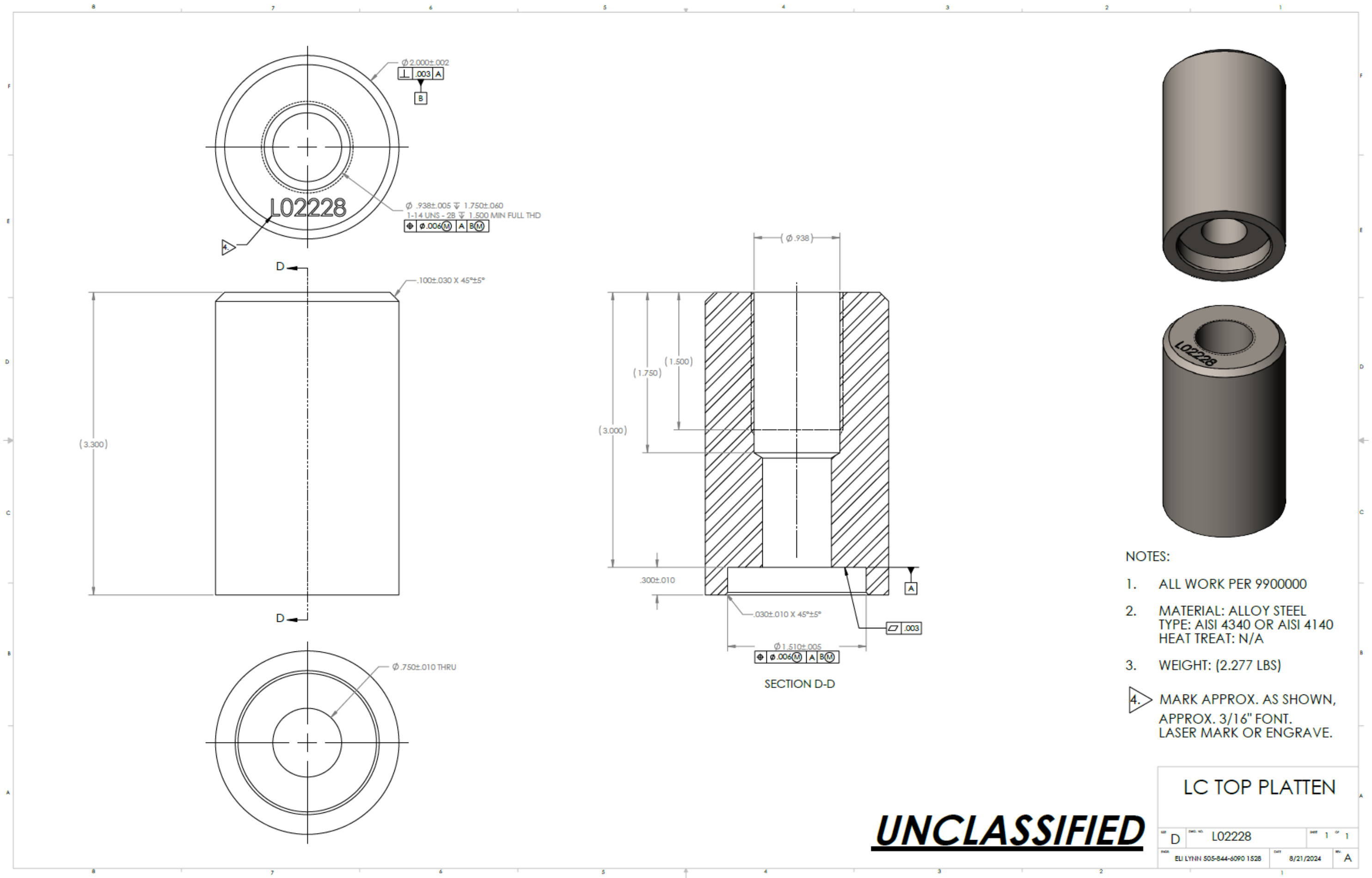

NOTES:

1. ALL WORK PER 9900000
2. MATERIAL: ALLOY STEEL
   TYPE: AISI 4340 OR AISI 4140
   HEAT TREAT: N/A
3. WEIGHT: (2.277 LBS)
4. MARK APPROX. AS SHOWN,
   APPROX. 3/16" FONT.
   LASER MARK OR ENGRAVE.

UNCLASSIFIED

LC TOP PLATTEN

D	L02228	1	1
ELI LYNN 505-844-6090 1528	8/21/2024	A	

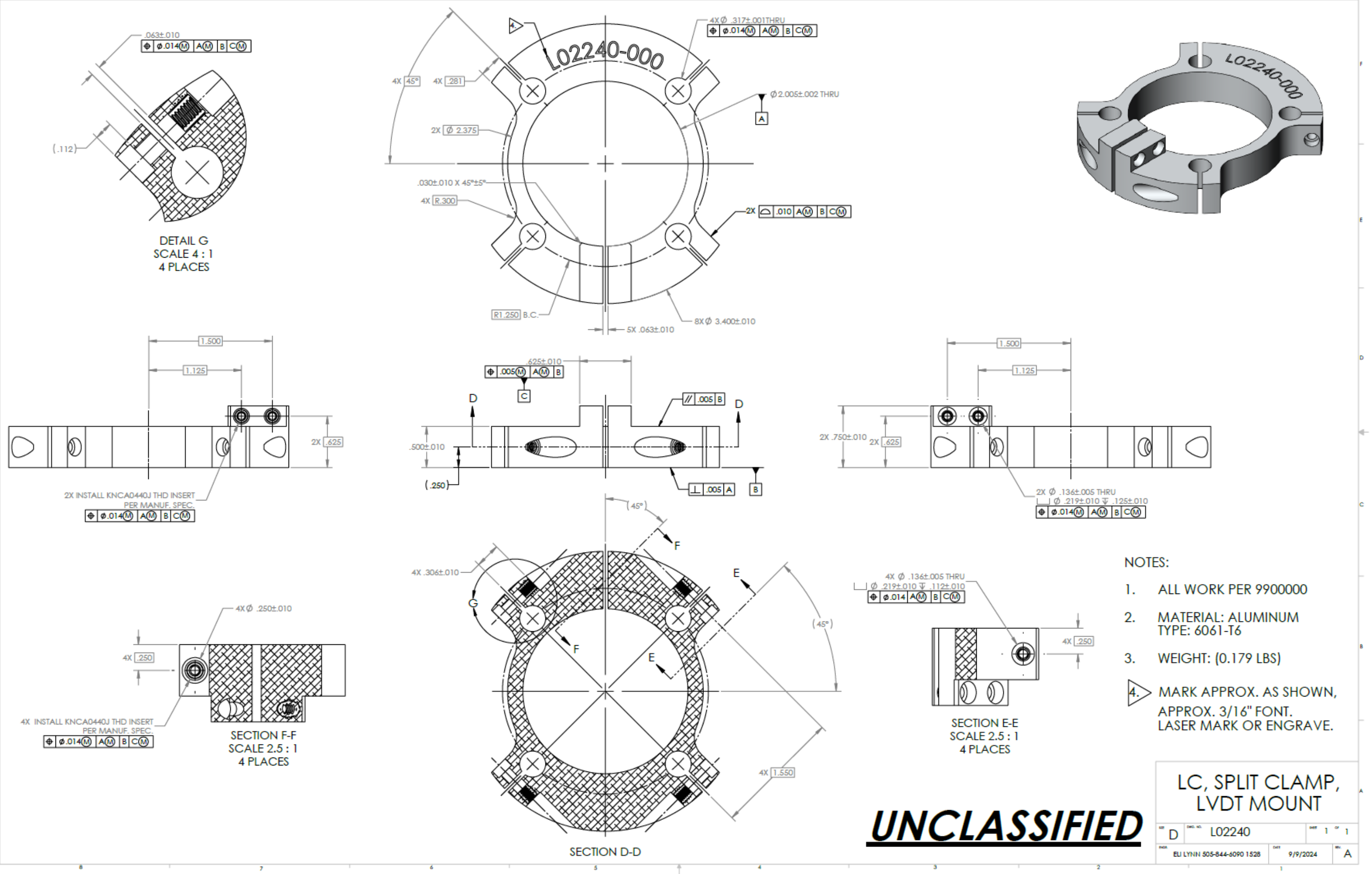

NOTES:

1. ALL WORK PER 9900000
2. MATERIAL: ALUMINUM
   TYPE: 6061-T6
3. WEIGHT: (0.179 LBS)
4. MARK APPROX. AS SHOWN,
   APPROX. 3/16" FONT.
   LASER MARK OR ENGRAVE.

UNCLASSIFIED

LC, SPLIT CLAMP,
LVDT MOUNT

D
L02240
1 1
ELI LYNN 505-844-6090 1528
9/9/2024
A

DISTRIBUTION

Email—Internal

Name	Org.	Sandia Email Address
Jessica Rimsza	8914	jrimsza@sandia.gov
Tina Nenoff	1000	tmnenof@sandia.gov
Harrison Root	1815	hdroot@sandia.gov
Sharlotte Kramer	1528	slkrame@sandia.gov
Kim Haulenbeek	1528	kkhaule@sandia.gov
Collin McConnell	1528	cemccon@sandia.gov
Timothy Elmslie	1879	taelmsl@sandia.gov
Nathan R. Bays	1852	nrbays@sandia.gov
Sakun Duwal	1646	sduwal@sandia.gov
Technical Library	1911	sanddocs@sandia.gov

Email—External

Name	Company Email Address	Company Name
Matthew J. Hurlock	matthew.hurlock@pnnl.gov	Pacific Northwest National Laboratories

This page left blank